ELSEVIER

Pattern Recognition Letters 16 (1995) 1033-1042

Pattern Recognition Letters

Point landmarks for registration of CT and MR images

S. Banerjee, D.P. Mukherjee, D. Dutta Majumdar *

Electronics and Communication Sciences Unit, Indian Statistical Institute, Calcutta 700035, India

Received 1 November 1994; revised 17 March 1995

Abstract

We propose here a point landmark based registration method utilizing geometric invariance properties of biomedical images. These point landmarks constitute entrance and exit points of concavities of individual structures and points of inflexion of curves, derived from the convex hull. Registration is performed in a canonical frame of reference. This technique is fast, semi-automatic and computationally inexpensive.

Keywords: Registration; point Landmarks; Concavities; Affine and projective transformations; Canonical frame; Measure of mismatch

1. Introduction

Registration is the process of determining a point-to-point correspondence between two images of the same object. This is a crucial first step for fusion of two image data sets to obtain an integrated image display. Applications include multimodality medical imaging (Banerjee and Dutta Majumder, 1993) and multisensor data fusion in remote sensing. Since images used in these applications are generally not well defined, the search for computationally inexpensive robust registration methods which require little or no expert interaction, constitutes an open problem in image processing.

In this paper we present our endeavors to develop a semi-automatic registration technique for 2D images which has been applied to register identical cross-sections of the human brain obtained from x-ray Computed Tomography (CT) and Magnetic Resonance (MR) modalities. Our method identifies point landmarks on surfaces of anatomical regions of interest (ROI) that are visible in all scans considered. These ROIs have a purely geometrical representation and can be extracted from the image by segmentation. The selection of such point landmarks is based on the geometrical invariance properties of the ROIs within the original image. Biomedical images possess a large number of concavities and we have used these concavities to locate landmark points or signatures.

This method can be classified (Van den Elsen et al., 1993) as a direct, semi-automatic method using a local or global transformation, depending on the number of structures of interest in the image and can be described as interpolating or approximating depending on whether three or more points are used. As we shall elaborate later, this point landmark based method possesses two distinct advantages over other point landmark based methods. The use of landmarks in images with geometric invariance properties simplifies the identification as well as automate the registration process. This method thus obviates the necessity of expert interaction (Hill et al., 1991) and hence results in a speed-up of computation. Secondly, this method does not require the computation of first and higher

* Corresponding author.

0167-8655/95/$09.50
SSDI 0167-8655(95)00058-5

order differentials of 3D image functions (cf. (Balter et al., 1992) and (Thirion et al., 1992)) which generally introduce noise in the image and are also computationally expensive.

The underlying Theory and Methodology that is used extensively for biomedical images, are described in the next section. In the succeeding section results of applying this technique to two sets of biomedical images (CT and MR) are given to illustrate the idea and a demonstration of the invariance properties is also included. The final section contains discussions of the advantages of this technique over others.

2. Methodology

The algorithm for image registration is as follows:

- *Generate a set of geometric invariants for different sub-contours of CT and MR images.* Contours or sub-contours (also the ROI's) which are *identical* in shape and structure have the same set of invariants. The converse is not necessarily true. However, invariants can usefully be used to generate hypotheses for matching, which could be verified subsequently. Like model based vision, absolute invariants are needed to propose a match. Invariants calculated locally to a sub-contour are used at this stage. This particular choice has the advantage that it does not depend globally on the curve. Consequently, if part of the curve is occluded or missed because of segmentation problems, local invariants can still be detected.
- *Locate possible "identical" sub-contours of CT and MR images based on matching pairs of geometric invariants.* Matching of invariants can be implemented as an $O(n)$ complexity process by the use of hashing (Rothwell et al., 1992), where n is the number of curves. We have implemented simpler $O(n^2)$ algorithm, since n is small in the case we have experimented with.
- *Verify the match of sub-contour pair in a canonical frame.* Having proposed matching curve pairs, we extract a set of point *landmarks* or *distinguished points* in the local sub-contour. These *landmarks* are curve inflexion points which could be distinguished irrespective of imaged transformations like rotation, scaling or shear. These are evaluated using any planar construction which is again preserved under projections. These *landmarks* are then used to transform the local sub-contour to a *canonical* frame. The verification that the curve pair (already hypothesized as a potential match) are identical is performed in the canonical frame. The ultimate goal of registration of images of two
- *Transformation of sub-contour in the canonical frame result in image registration.* The registration of contours of two different modalities in the canonical frame gives the amount of mismatch (both locally for sub-contours or globally for the entire edge image) between the two data set. This can as well be used as an indication of a biological growth or missing of a subpart of an organ or structure of interest.

We have largely considered the concavities present in the ventricle of human brain as local sub-contours or ROI. The implementation details including its (ROI) detection, calculation of geometric invariance and finally transformation of ROI onto canonical frame is detailed in the next section.

3. Implementation

Detection of concavity. Planar CT and MR image slices are subjected to a local implementation of Canny (1986) edge operator followed by edge linking. We have largely exploited the concavities present in the ventricle of human brain to detect the point *landmarks*. The entire edge point set is traced by an edge following algorithm (Ballard and Brown, 1982) and the coordinates of these points are stored in a file. Significant concavities are extracted for each closed contour after computing a convex hull and setting a threshold on concavity height and width.

Concavity landmark *points.* Evaluation of convex hull on the edgel data set of the CT or MR images gives concavity entrance and exit points of a significant concavity. Also, the point on the concavity which is furthest from the bitangent connecting concavity entrance and exit points gives the concavity height point. In case of more than one concavity height points, the ambiguity is resolved taking the leftmost of the concavity height point set. The concavity entrance, exit and height points are *invariant landmarks*. These three point set gives a stable construction

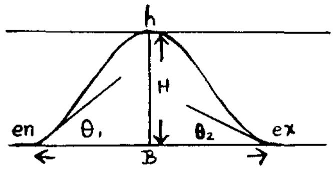

Fig. 1. *en*, *ex* and *h* are the concavity entrance, exit and height points respectively for a significant concavity. The ratio H/B, angles θ_1 and θ_2 are the ratio-angle-angle invariant triplet (up to similarity transform) used for concavity matching.

which could be used for subsequent concavity matching/registration of images of different modalities.

A set of geometric invariants, upto similarity transform, is evaluated to generate hypotheses for a potential match. The ratio of concavity height to concavity width, the angle(s) between the lines connecting concavity entrance (and exit) point(s) and the concavity height point to the line joining concavity entrance and exit points give ratio-angle-angle invariant triplets. The ratio H/B, angles θ_1 and θ_2, as in Fig. 1, are the ratio-angle-angle invariant triplet (upto similarity transform) used for concavity matching. These are used to find the matching concavity set between the CT and MR image sets.

Mapping onto canonical frame. A planar affine model similar to Mukherjee et al. (1993) is used to match the concavities in the canonical frame. An affine transformation maps a straight line onto a straight line (collineation) while preserving parallelism. This is a linear transformation with six degrees of freedom due to translation, rotation, scaling and shear or unequal scaling along the axes. A 2D affine transformation on a vector $\boldsymbol{x}$ onto X is represented by

$$X = A\boldsymbol{x} + \boldsymbol{t} \tag{1}$$

where A is a 2×2 transformation matrix representing rotation, overall scaling and shear. Vector $\boldsymbol{t}$ is a 2D translation vector. There are six unknowns, corresponding to four coefficients of the transformation A and two translation vector coefficients. Significant concavities are transformed to a triangular canonical frame with vertices at $(-100, 0)$, $(100, 0)$ and $(0, 100\sqrt{3})$ by using the point landmarks or affine basis triplets of the concavity. The elements of A and $\boldsymbol{t}$ are evaluated following equation (1) and the entire edgel set of the CT or MR image contour is transformed to the canonical frame.

For a certain set of images, as in Fig. 2, depending upon features of concavity e.g. concavity height and width, a projective model is used to transform the concavity onto the canonical frame. In this case, the transformation is represented by

$$\boldsymbol{X} = T\boldsymbol{x} \tag{2}$$

where T is a 3×3 projective transformation matrix with eight degrees of freedom [1]. Both vectors $\boldsymbol{x}$ and X are represented in homogeneous coordinates. Quite straightforwardly, we need four points to evaluate matrix T. The square canonical frame, therefore, has four vertices at $(-100, -100)$, $(-100, 100)$, $(100, 100)$ and $(100, -100)$.

In order to verify the match between the transformed concavities, a further set of invariants are calculated in the canonical frame. We have determined moments (both about x and y-axis) of the transformed concavity pair. The matching concavity pairs have their invariant values close to $\pm 5\%$. Once this registration of CT and MR images are established in the canonical frame, moments of the entire contours are calculated to evaluate the global match (or the amount of mismatch) between the data of two different modalities. The result in the tabular form is shown in Table 1.

The measure of mismatch between the two images has been computed as follows. Centroids of the images of the two modalities have been computed with respect to the particular canonical frame of reference. The difference in this value of one image with respect to the other is computed. Centroids of individual concavities have been computed similarly. Other measures of mismatch are also possible.

4. Experiment

Digitized images of axial sections of the the same region of the human brain of the same patient obtained from MRI (Magnetic Resonance Imaging) and CT (Computed Tomography) modalities are used. These images contain 512×512 pixels per slice. For the two images under consideration (see Figs. 2 and 3),

[1] The eight degrees of freedom arise from the nine matrix elements of T, less an overall scale factor.

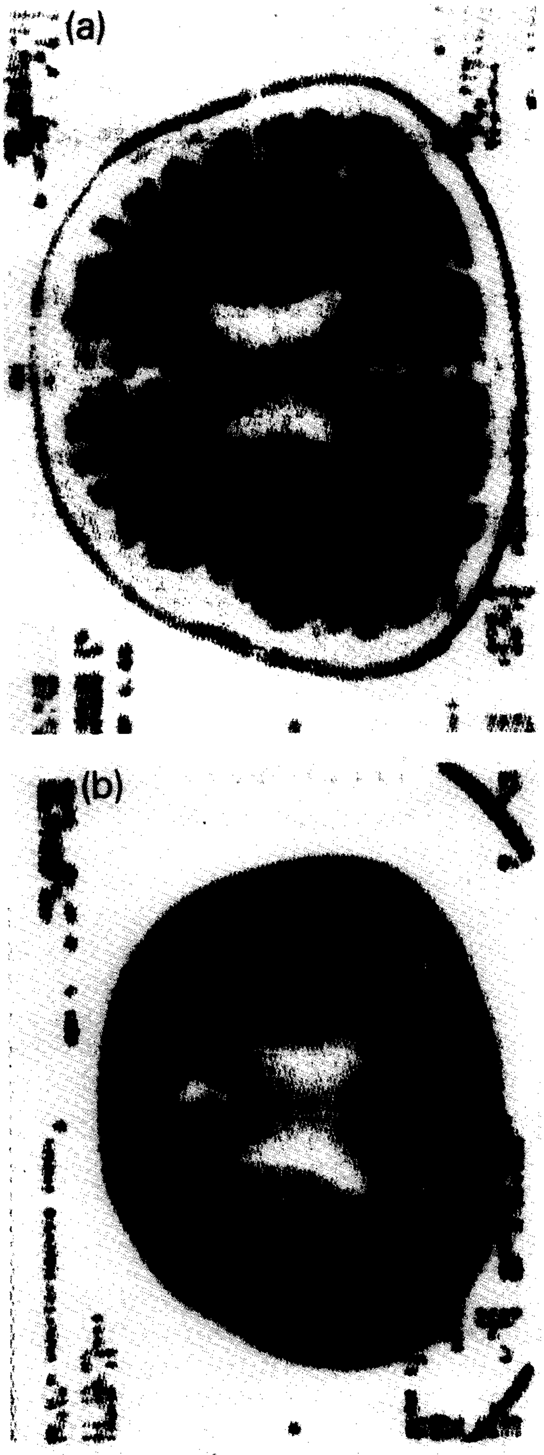

Fig. 2. Axial section of brain for (a) CT and (b) MRI modalities, containing two structures of interest.

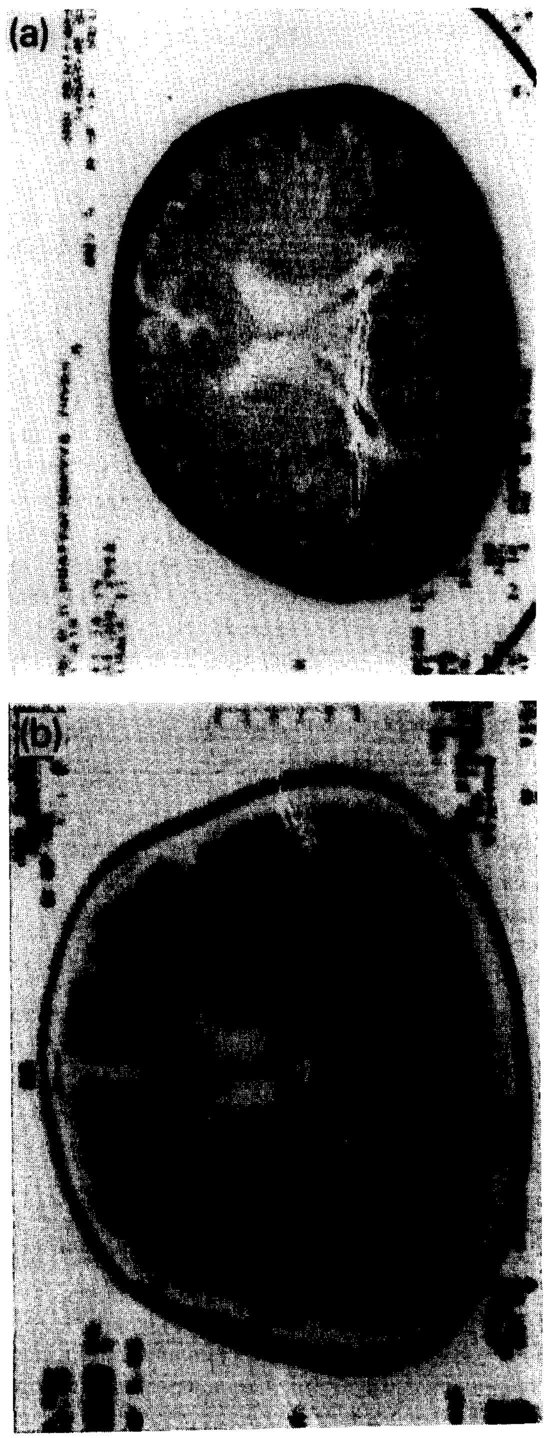

Fig. 3. Axial section of brain for (a) CT and (b) MRI modalities, containing one structure of interest.

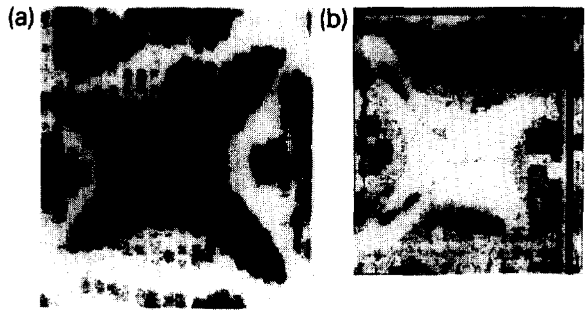

Fig. 4. Region of interest for (a) CT and (b) MRI images extracted from Fig. 2 (N.B. ROI in MRI is inverted w.r.t. CT image).

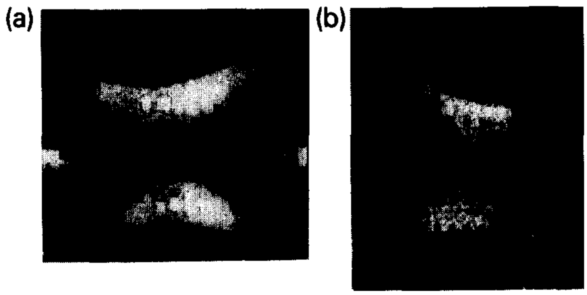

Fig. 5. ROI for (a) CT and (b) MRI images extracted from Fig. 4 (N.B. ROI in MRI image is inverted w.r.t. CT image).

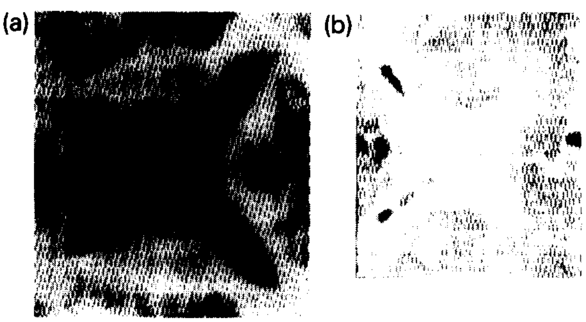

Fig. 6. Smoothed images of Fig. 4 for (a) CT and (b) MRI modalities.

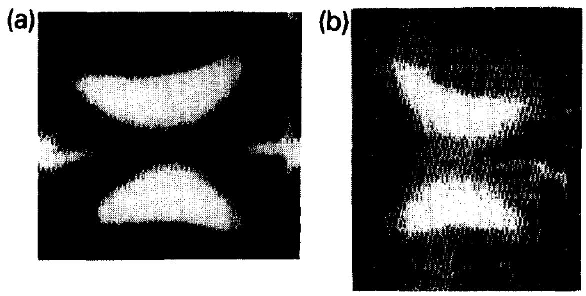

Fig. 7. Smoothed images of Fig. 5 for (a) CT and (b) MRI modalities.

Table 1
Comparison of mismatch using local "footprint" or global measure
Notation: i: inner, o: outer, l,L: left, r,R: right, T: top, B: bottom

Figure	Local		Global	
	Moment (x)	Moment (y)	Moment (x)	Moment (y)
8(a) CT-il	44.78	48.08	92.36	54.22
8(a) CT-ir	76.47	58.13	-	-
8(a) CT-ol	26.11	53.50	-	-
8(a) CT-or	92.90	48.70	-	-
8(b) MR-il	36.03	37.62	89.99	54.48
8(b) MR-ir	70.60	12.64	-	-
8(b) MR-ol	13.70	36.50	-	-
8(b) MR-or	86.47	39.50	-	-
9(a) CT-L	51.79	111.47	53.18	285.98
9(a) CT-R	51.61	91.92	-	-
9(a) CT-T	51.09	98.92	-	-
9(a) CT-B	50.98	91.63	-	-
9(b) MR- L	50.82	97.71	56.83	288.76
9(b) MR-R	50.68	97.27	-	-
9(b) MR-T	51.16	93.92	-	-
9(b) MR-B	50.18	86.07	-	-

Table 2
Image parameters for the images of Figs. 6 and 7

Figure	Modality	Dimensions (pixels) of image	Grey-level threshold (0–255)
6(a)	CT	132 × 107	171
6(b)	MRI	117 × 122	129
7(a)	CT	132 × 112	219
7(b)	MRI	152 × 137	116

the ventricle is chosen as the ROI (Figs. 4 and 5). These images are smoothed, thresholded and edges are extracted using Canny's (1986) edge detection algorithm with a sigma value of 7. Details of images of these regions of interest are given in Table 2. The smoothed images of the ROIs are shown in Figs. 6 and 7, respectively. Edges of these images are extracted after thresholding.

After edge extraction, entrance and exit points of the concavities as well as the points of inflexion are obtained from the convex hull. These points, as well as the heights and widths of the concavities for the two sets of images for both the modalities are depicted in Figs. 8 and 9. Ratios of the heights to the widths are computed for the concavities and Fig. 10 represents an axial MRI section of a different patient. Fig. 11 represents the edge image of a significant portion of Fig. 10. Fig. 12 represent the image of Fig. 11 scaled down by a factor of 1.5. Landmark points corresponding to the three concavities are depicted in Figs. 11 and 12.

For each of the images of the image set contain-

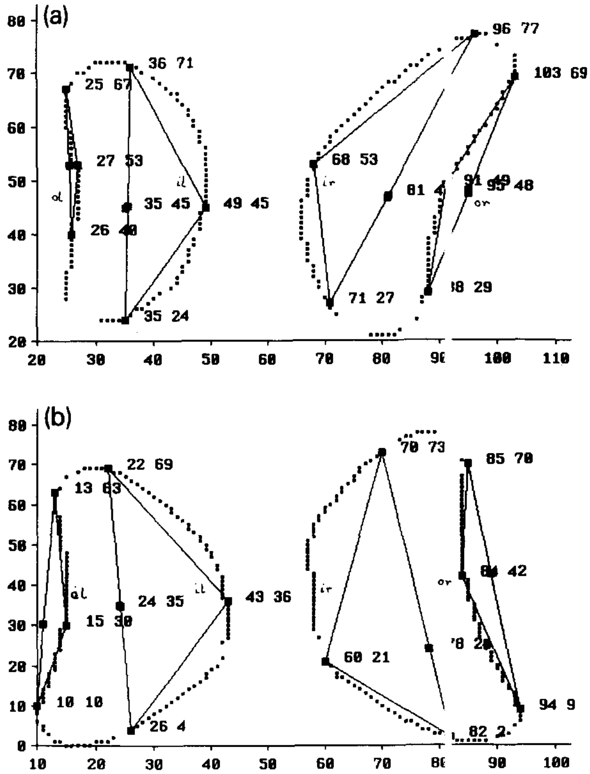

Fig. 8. Landmark points of Fig. 6 for (a) CT and (b) MRI images. (N.B. Due to tear in the contour of the right structure, signatures corresponding to its inner concavity have been extracted from the unbroken portion for both the images.)

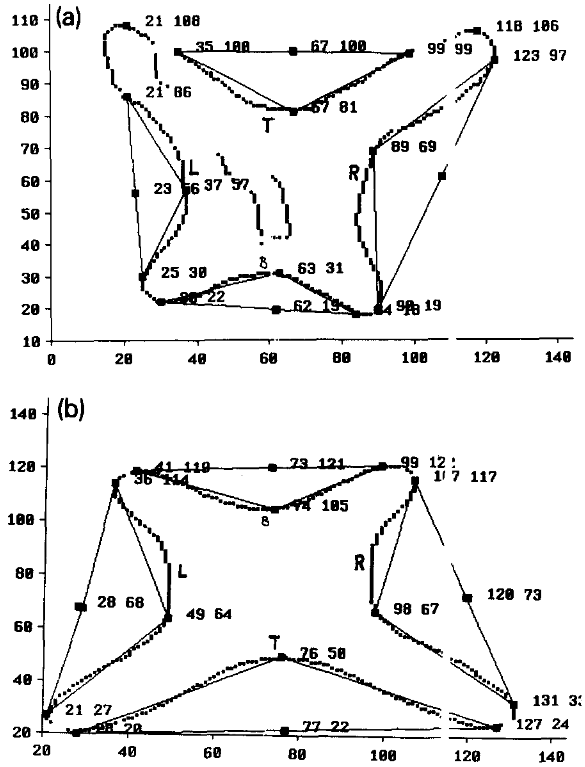

Fig. 9. Landmark points of Fig. 8 for (a) CT and (b) MRI images. (For (b), there is a tear in the edge along the top concavity, so the footprints have been extracted from the unbroken edge.)

ing one structure of interest (Fig. 9), one concavity is chosen (we have chosen the largest one by visual inspection) and a local affine transformation to a canonical frame is performed, thus mapping the three points which correspond to the entrance, highest and exit points of the concavity, to the three vertices $(-100, 0)$, $(0, 100\sqrt{3})$ and $(100, 0)$ of an equilateral triangle in the canonical frame, shown in Fig. 13.

Fig. 14 depicts a canonical frame of reference in which both the images of Fig. 8 are superimposed after a global projective transformation is performed on each of them. The two entrance and exit points of the inner concavities of both the images in Fig. 8 are chosen as the four points required for the projective transformation. These points correspond to $(-100, -100)$, $(-100, 100)$, $(100, 100)$ and $(100, -100)$ in the canonical frame. Other choices of points are also possible. The result of applying a local affine transformation similar to Fig. 13 to image set of Fig. 9

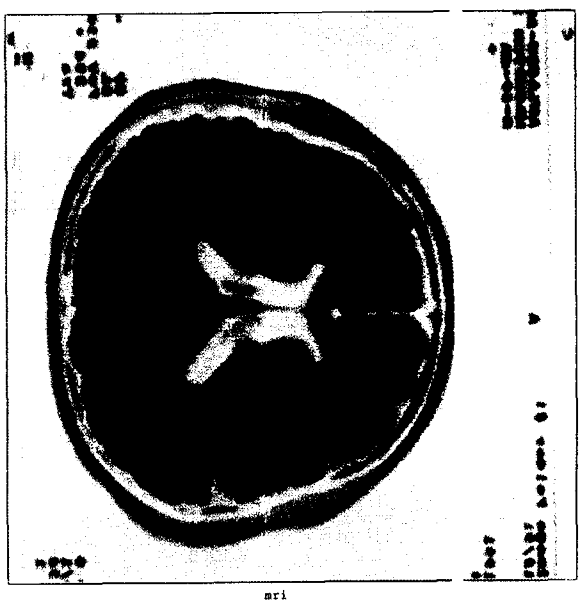

Fig. 10. Axial MRI section of a different patient.

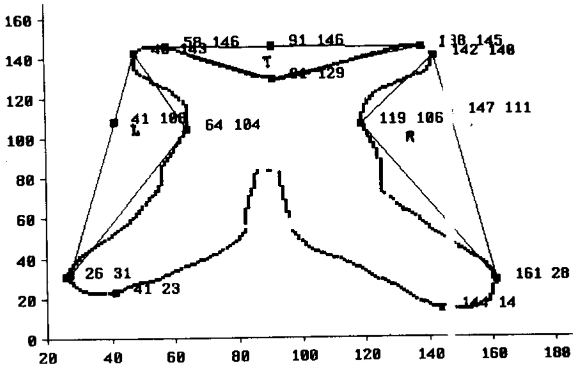

Fig. 11. Edge image of significant portion of MRI image (pixel dimension: 172 × 152) extracted from Fig. 10.

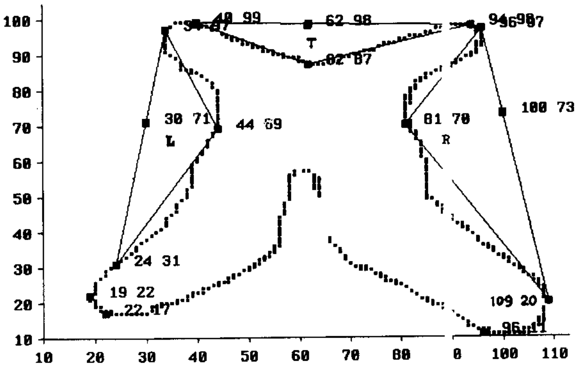

Fig. 12. Fig. 11 scaled uniformly (decreased by a factor of 0.66) (pixel dimension 114 × 101).

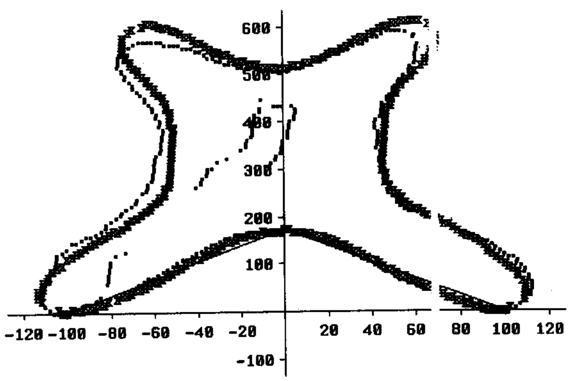

Fig. 13. Canonical frame containing superposed CT and MRI images of Fig. 9 after an affine transformation.

with the entrance, height and exit points of the inner concavity of the left structure, is presented in Fig. 15.

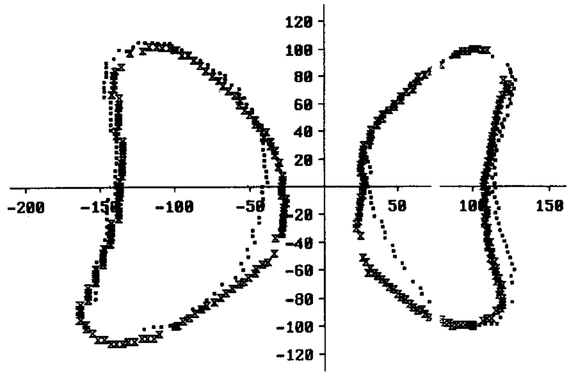

Fig. 14. Canonical frame containing superposed CT and MRI images of Fig. 8 after a projective transformation.

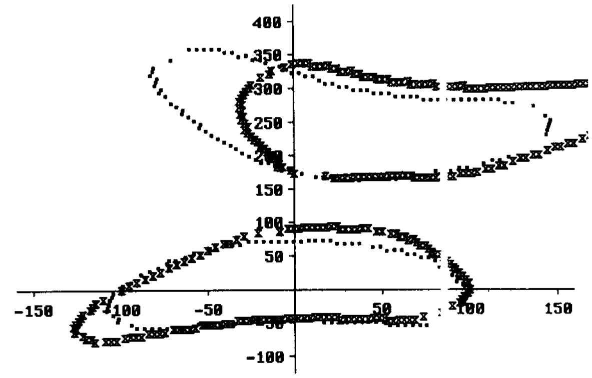

Fig. 15. Canonical frame containing superposed CT and MRI images of Fig. 8 after an affine transformation.

4.1. Results

Tables 3 and 4 present values of the ratios of their heights to widths and the percentage of difference for both the image sets of the two modalities. This difference is small, indicating that there is good agreement. Fig. 13 shows a superposition of the images of Fig. 8 after a local affine transformation and Fig. 14 represents the superposition of Fig. 9 after a global projective transformation. From Fig. 15 it is evident that a local affine transformation which suffices to map an individual structure containing the three signature points, becomes inadequate when the image contains several structures. A global transformation is recommended in such situations. An inspection of table 1 reveals that a reasonably good match has been obtained as the measure of mismatch is small. This measure of mismatch is computed as the deviation of the centroid

Table 3
Landmarks and invariants of Fig. 8 (2 structures)
Number of concavities = 2 outside structures and = 2 inside structures, total = 4

Figure	Modality	Concavity	Height	Width	Ratio (height/ width)	Comments
8(a)	CT	il	13.55	47.01	0.29	-
		ol	1.48	27.02	0.055	-
		ir	14.31	55.9	0.26	-
		or	4.21	42.72	0.1	-
8(b)	MRI	il	18.93	69.01	0.36	80 % agreement w/CT.
		ol	3.86	53.1	0.07	79 % agreement
		ir	18.53	72.01	0.28	93 % agreement
		or	5.08	61.66	0.08	80 % agreement

Table 4
Landmarks and invariants of Fig. 9 (1 structure)
Number of concavities = 4 outside structure

Figure	Modality	Concavity	Height	Width	Ratio (height/width)	Comments
9(a)	CT	L	13.89	56.15	0.25	-
		R	20.4	84.89	0.24	-
		T	18.5	64.01	0.29	-
		B	11.41	54.15	0.21	-
9(b)	MRI	L	21.31	88.28	0.24	94 % agreement w/CT
		R	22.39	87.36	0.26	92% agreement
		T	15.69	58.08	0.27	77 % agreement
		B	28.04	99.08	0.28	95 % agreement

of the CT image from the MRI image with respect to the MRI image. From Table 5, one can conclude that these landmark points are scale invariant.

5. Discussions

We have chosen patient intrinsic markers in our registration technique. Object intrinsic markers are preferred over extrinsic ones for better accuracy and retrospective viewing of images. Several registration techniques using object intrinsic markers are being explored (Van den Elsen et al., 1993) in biomedical imaging. These markers can be points (Chen et al., 1985; Boesecke et al., 1990; Balter et al., 1992; Thirion, 1993), centroids of segmented regions (Bartoo et al., 1989), contours (Van den Elsen et al., 1994; Thirion et al., 1992), surfaces (Gamboa-Aldeco et al., 1986; Pelizzari et al., 1989; Collignon et al., 1994) or user-identified point like anatomical features (Hill et al., 1991), to mention a few. Of these, methods based on centroid determination are good only in the absence of occlusion. Surface based registration algorithms are meaningful when there is proper correspondence information between the two images and the image has been treated for the removal of outliers. Signature points are required to establish correspondence in contour based matching (Balter et al., 1992). Point landmarks are also useful in reducing the lack of correspondence information in surface registration (Collignon et al., 1994).

Our method is essentially a point landmark based technique which does not require differentials of image functions and is therefore more robust, and based on geometrical invariance properties and thus the necessity of expert interaction is minimized. Recently, a number of point landmark based registration methods have been reported. Hill et al. (1991) have performed registration of MR and CT images using anatomical point like features. This method requires extensive user interaction by a clinician for identification of such landmark points since such landmarks are endemic to the organ/ structure of interest. This is an extremely time consuming process. Point landmarks with geometric invariance properties simplify identification as well as automate the registration process. Thirion (1993) uses feature points based on geometric invariance of images under translation and rotation, for registration. These feature points are referred to as extremal points and correspond to the intersection of the zero-crossings of the first-order directional derivatives of the two principal curvatures with iso-

Table 5
Landmarks and invariants of Fig. 10 (1 structure)
Number of concavities chosen = 3 outside structure

Figure	Modality	Concavity	Height	Width	Ratio of height to width	Comments
11	MRI (172 × 152)	L	22.97	112.97	0.20	-
		Right	28.36	113.56	0.25	-
		T	16.59	80.0	0.21	-
12	MRI (114 × 101)	L	14.1	66.75	0.21	95 % agreement w/11
		R	19.29	78.09	0.25	100 % agreement
		T	11.59	54.01	0.21	100 % agreement

intensity surfaces of a 3D image. Crest lines are loci of iso-intensity surfaces where the extremal curvature is locally maximal and these lines have also been used for registration (Thirion et al., 1992). These methods utilize first- and second-order differentials of the 3D image functions which are computed with linear filtering using the convolution of the discrete image with the differential of the gaussian function to calculate principal curvatures and principal directions. Elsen et al. (1994) have formulated an automated approach to register CT and MR brain images exploiting geometric invariance, by applying differential operators in scale space to each type of image data to produce feature images depicting "ridgeness". Balter et al. (1992) have devised a landmark based registration technique for 2D images that matches contours corresponding to projections of curved surfaces from similar images which have some degree of overlap. After determining the optimal overlap by parametrizing contours by their arclength and computing local curvatures, the curves are sampled over their common regions giving corresponding sets of points. In all these geometry based methods, curves (2D) or surfaces (3D) are extracted from the image and curvatures computed from the first and second derivatives of the image. From a computational point of view, this is labour intensive. The digital implementation of second order differential operators introduces noise in the images which have to be subsequently removed. The method we propose here also locates characteristic points having geometric invariance under rotation, translation and scaling, for registration of planar images of different modalities in a common frame of reference referred to as the canonical frame. Our method does not require the computation of image derivatives.

The landmark based technique that we have detailed in the preceding sections is fast, computationally inexpensive and requires minimal user interaction. This technique works best when edges of images are well defined and it is possible to choose concavities for which the edges comprise of clear, unbroken contours. Biomedical images generally have complex structures containing a number of concavities, some of whose edges are hazy and sometimes occluded, and so, the user will have to select suitable edges. When broken/torn edges have to be used one can either resort to edge linking techniques or the user needs to select the unbroken portion of the contour manually to extract the entrance/exit points. Another aspect which entails user interaction is the choice of transformation to be performed to bring the images to a canonical frame. This, off course, depends on the number of structures to be viewed. The choice of point pairs in projective transformation should be guided by the location, importance and rigidity of the anatomical structures of interest.

Ventricles of the brain are also prominent in functional images like Positron Emission Tomography and Single Photon Emission Computed Tomography. Concavities in axial images of these modalities appear as valleys between hills in an intensity landscape. The technique outlined above is thus applicable for the registration of such functional images with morphological ones (CT, MRI). The possibility of extending this technique to 3D is currently under investigation.

Acknowledgments

Two of us (SB, DDM) wish to acknowledge funding from CSIR, India. We thank Andrew Zisserman and Mike Brady for their thoughtful suggestions. We would like to thank JMD Medicare and Siemens Ltd., both of Calcutta for kindly providing us with the images.

References

Arun, K.S., T.S. Huang and S.D. Blostein (1987). Least-squares fitting of two 3-D point sets. *IEEE Trans. Pattern Anal. Mach. Intell.* 9 (5), 698–700.

Ballard, D.H. and C.M. Brown (1982). *Computer Vision.* Prentice-Hall, Englewood Cliffs, NJ, 131–146.

Balter, J., G.T.Y. Chen, C. Pelizzari and D.S. Fritsch (1992). A multiple landmark interface for image registration in radiotherapy. *Second Internat. Workshop on Electronic Portal Imaging* (Abstract).

Banerjee, S. and D. Dutta Majumdar (1993). A medical expert system using multimodality imaging. *Proc. Internat. Conf. Pattern Recognition and Digital Techniques, ICAPRDT '93*, Calcutta, India, Dec. 1993, 493–499.

Bartoo, G.T. and W.A. Hanson (1989). Multimodality image registration using centroid mapping. *Proc. IEEE Internat. Conf. Engg. Med. Biol. Soc.*, 550–551.

Boesecke, R., T. Bruckner and G. Ende (1990). Landmark based correlation of medical images. *Phys. Med. Biol.* 35, 121–126.

Canny, J.F. (1986). A computational approach to edge detection. *IEEE Trans. Pattern Anal. Mach. Intell.* 8 (6), 679–698.

Chen, G.T.Y., M. Kessler and S. Pitluck (1985). Structure transfer between sets of three dimensional medical imaging data. *Proc. Computer Graphics*, 171–177.

Collignon, A., D. Vandermeulen, P. Seutens and G. Marchal (1994). Registration of 3D multi-modality medical imaging using surfaces and point landmarks. *Pattern Recognition Lett.* 15, 461–467.

Gamboa-Aldeco, A., L.L. Fellingham and G.T.Y. Chen (1986). Correlation of 3D surfaces from multiple modalities in medical imaging. *Proc. Soc. Photo Optical Eng.* 626, 467–473.

Hill, D.L.G., D.J. Hawkes, J.E. Crossman, M.J. Gleeson, T.C.S. Cox, E.E. Bracey, A.J. Strong and P. Groves (1991). Registration of MR and CT images for skull base surgery using point like anatomical features. *Brit. J. Radiol.* 64, 1030–1035.

Mukherjee, D.P., A. Zisserman and M. Brady (1993). Shape from symmetry – Detecting and exploiting symmetry in affine images. *Proc. Roy. Soc. Ser. A*, in press.

Pelizzari, C.A., G.T.Y. Chen, D.R. Spelbring, R.R. Weichselbaum and C.T. Chen (1989). Accurate three dimensional registration of CT, PET and/or MR images of the brain. *J. Comp. Assist. Tomogr.* 13, 20–26.

Rothwell, C.A., A. Zisserman, D.A. Forsyth and J.L. Mundy (1992) Canonical frames for planar object recognition. In: *Proc. ECCV2.* Springer, Berlin, 757–772.

Thirion, J.P. (1993). New feature points based on geometric invariants for 3D image registration. INRIA Research Report No. 1901.

Thirion, J.P., O. Monga, S. Benayoun, A. Gueziec and N. Ayache (1992). Automatic registration of 3D images using surface curvature. *IEEE Internat. Symp. on Optical Applied Science and Engineering*, San Diego, CA, July 1992.

Van den Elsen, P.A., E.J.D. Pol and M.A. Viergever (1993). Medical image matching – A review with classification. *IEEE Trans. Engg. Med. Biol.*, 26–39.

Van den Elsen, P.A., J.B.A. Maintz and M.A. Viergever (1994). Automatic registration of CT and MR brain images using correlation of geometric features. Submitted to *IEEE Trans. Med. Imaging.*